Open Access

Journal of Energy and Power Technology

LIDSEN Publishing Inc.

Original Research

Study of Hydrogen Embrittlement in Pipelines and Nuclear Power Plants: Estimates for Durability

Alla V. Balueva [1,*], Ilia N. Dashevskiy [2], Christian Sims [1]

1. Mathematics Department, University of North Georgia, P.O. Box 1358, Gainesville, Georgia 30503, USA; E-Mails: Alla.Balueva@ung.edu; Christian.Sims@ung.edu
2. Ishlinsky Institute for Problems in Mechanics RAS, pr. Vernadskogo, 101-1, 119526 Moscow, Russia; E-Mail: dash@ipmnet.ru

* **Correspondence:** Alla V. Balueva; E-Mail: Alla.Balueva@ung.edu

Academic Editor: Zhao Yang Dong

Journal of Energy and Power Technology
2022, volume 4, issue 3
doi:10.21926/jept.2203028

Received: April 18, 2022
Accepted: June 19, 2022
Published: August 30, 2022

Abstract

Due to the increasing need to further develop the world gas and oil industry and the increased public attention to clean energy sources, studying and preventing Hydrogen Induced Cracking is one of the main safety concerns in nuclear power plants, oil pipelines and platforms. In this article, the growth and incubation times for internal Hydrogen Induced Cracks (HIC) are examined. Specifically, these times are modeled in two separate phases - the first phase (I) is a long time approximation, when the crack growth is believed to be slow such that the equilibrium state for gas concentration establishes instantaneously, and the stationary diffusion problem can be solved for each moment of time. The second phase (II) is a short time approximation, when the crack growth is rapid and the concentration of atomic hydrogen is dependent on time. Closed-form solutions are obtained in both cases and are then coupled using a Padé approximation.

Keywords

Hydrogen induced cracking; multi-phase crack growth; closed-form solutions; Padé approximation

1. Introduction

Hydrogen embrittlement – also referred to as hydrogen induced internal cracks or hydrogen delamination – is a well-documented and much-observed process that impacts many kinds of metals in a hydrogen saturated environment (e.g., [1-6]). The negative effects of hydrogen embrittlement include internal and external blistering, which lead to decreased load, tension, and stress capacities [1, 4, 7, 8]. Hydrogen embrittlement also leads to the failing and bursting of metal components such as pipes and boiler tubes (e.g. Figure 1 and Figure 2) [9-11], and decreased efficiency in nuclear fusion reactors [12, 13].

Figure 1 Sudden rupture of oil pipeline (Wikipedia).

Figure 2 Hydrogen induced cracking of pipeline (Wikipedia).

A recent Wall Street Journal review (Wikipedia) found that there were 1,400 pipeline spills and accidents in the U.S. between 2010 and 2013 due to defective pipelines. Our research will provide oil engineers with simple and robust formulas that can be used to estimate when defective pipeline should be replaced. This will help reduce spills and accidents that cause property damage and worker fatalities.

Multiple factors effect hydrogen embrittlement, including crystallographic orientations, grain boundaries, dislocations, and hydrogen trapping (e.g., [1, 4, 8, 11, 14, 15]). The orientation and layout of grain boundaries have a significant impact on crack formation, especially since deformations and cavities are often positioned along the grain boundaries (e.g., [1, 8, 16, 17]). Hydrogen diffuses through the material and collects at these vulnerable points, leading directly to internal cracks [18]. Hydrogen embrittlement has been investigated in numerous ways and in many contexts. Many experiments focus on piping and boiler tubes, since these are the most common victims of hydrogen embrittlement [9-11, 19]. Hydrogen embrittlement is a huge obstacle for

hydrogen fusion research, since the interiors of tokamaks are bombarded with hydrogen [4, 12, 13]. Many experiments are performed to test the susceptibility of certain metals to hydrogen embrittlement [3-5, 10, 20].

Multiple phenomenological models have been put forward to describe hydrogen embrittlement, each focusing on specific aspects of the problem (e.g., [21-24]). Benannoune et al. [12] proposed a model based on a generalized version of Oriani's Approximation for hydrogen trapping that simulates hydrogen charging and discharging in materials. Martinez-Paneda et al. [25] developed a model that predicts crack growth and failure stress sensitivity based on hydrogen diffusion, chemical potential gradients, and first principles calculations. Gibala et al. [17] examine various factors for developing analytical models, and they give an equation for finding the number of vacancy traps for hydrogen in a given material based on its molecular structure. Huang et al. [26] give a model that quantifies hydrogen embrittlement by evaluating the coalescence of small fractures.

Toribio and Kharin [27] developed a model that is centered around the concentration of hydrogen in the metal, since cracks occur when this concentration reaches a critical point. They examined the hydrogen concentration by looking at grain and crystal irregularities, which affect the diffusion of hydrogen and cause it to deviate from Fickian behavior. Their model combines several known diffusion models into a continuous model based on random-walk theory.

Wu et al. [28] offer a coupled model for the kinetics of crack growth in phases I and II as the stress intensity factor (SIF) increases. Both phases are influenced by hydrogen diffusion, but the rate of crack growth, da/dt, increases steeply in phase I and is nearly linear in phase II. They explain this difference as a change in the SIF K_I. In analyzing crack growth, they base their model off the gradient of the chemical potential μ, linear-elastic fracture mechanics, and the velocity of a hydrogen atom. The chemical potential is important since it determines hydrogen diffusion and thus crack growth in all phases. Fracture mechanics provides the background or field in which the crack occurs. Their proposed coupled model for the rate of crack growth is proportional to the change in the SIF and the length of the crack. As with several other models mentioned above, their model fits with experimental data.

The models described above give good explanation and description to the processes during Hydrogen Embrittlement. However, due to the complexity of the phenomenon, not too many works are available, which give exact analytical solutions at the end. The work presented in this paper proceeds directly from that conducted previously [29-31]. In the former works, an analytical model of the *surface* crack, or *delamination*, growth was presented. In the present paper an analytical model for *internal* HIC growth is introduced and closed-form solutions for crack growth times in long- and short-time approximations are obtained, which will give simple and robust estimates for the longevity of equipment operating in harsh hydrogen-saturated environments.

2. Internal Crack Growth under Hydrogen Diffusion

Let us consider an internal crack with a penny-shaped form, having an initial radius a_0 in infinite media, which is saturated with gas of concentration c_0 (Figure 3). In the material, gas is in atomic form, and it diffuses into places of high stress concentration, usually small voids and cracks. Inside these cracks it reforms into molecular form, and if the gas pressure is not too high, it gets trapped and starts accumulating there (Figure 3).

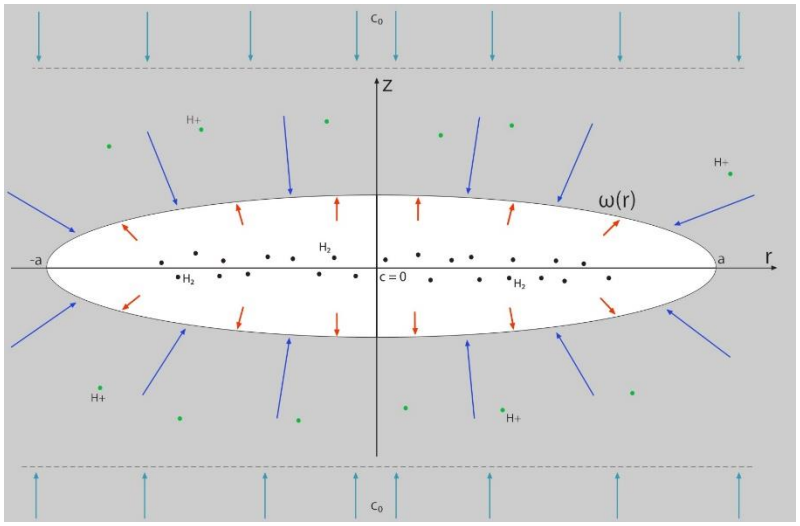

Figure 3 Mechanism of hydrogen induced cracking.

When gas pressure reaches the value at which the critical conditions at the crack contour are met

$$K_{Ic} = 2p\sqrt{\frac{a}{\pi}} \tag{1}$$

then the crack starts growing. Taking into account equation (1) and the relation between the critical stress intensity factor, K_{Ic}, and the critical surface energy, γ_c, the expression for the gas pressure p can be expressed as:

$$2\gamma_c = \frac{(1-\nu^2){K_{Ic}}^2}{E} = \frac{(1-\nu^2)4p^2}{E}\frac{a}{\pi} \tag{2}$$

or

$$p^2 = \frac{2\gamma_c \pi E}{4(1-\nu^2)a} \tag{3}$$

The volume of the crack, the gas pressure, and gas mass are connected through the gas state equation:

$$pV = mRT \tag{4}$$

where R = 8.314 J/(mole × °K) is the ideal gas constant.

If the crack volume increases, the gas pressure drops according to (4), and the critical stress conditions are not met at the crack contour. Thus, the crack stops growing, waiting for new gas accumulation (Figure 4). This is why hydrogen induced cracking typically occurs at a very slow speed.

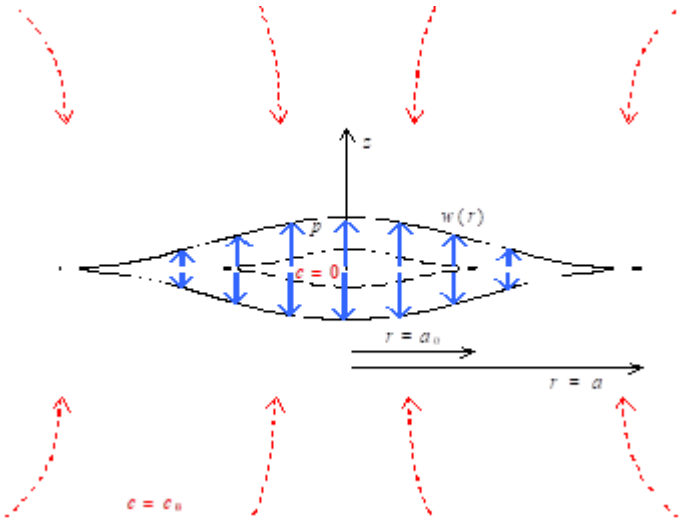

Figure 4 Internal crack growth under the pressure of gas accumulated in the crack.

The crack aperture for the internal crack can be written as

$$w(r) = \frac{4(1-\nu^2)p}{E\pi}(a^2 - r^2)^{\frac{1}{2}} \tag{5}$$

and we can find the volume *V* of the crack by integrating (5) over the crack area

$$V = \frac{16(1-\nu^2)pa^3}{3E} \tag{6}$$

To obtain a kinetic equation for the crack radius *a(t)*, the expressions for the gas pressure *p* from (2), (3) and the volume *V* (6) in terms of a are substituted into the gas state equation (4):

$$a^2\gamma_c = \frac{3RT}{4\pi}\int_0^t Q(a(t),t)\,dt \tag{7}$$

where $Q(a(t),t)$ is the full gas flux into the crack and can be found from the gas diffusion problem:

$$\begin{cases} \dfrac{\partial c}{\partial t} = D\left[\dfrac{\partial^2 c}{\partial z^2} + \dfrac{1}{r}\dfrac{\partial}{\partial r}\left(r\dfrac{\partial c}{\partial r}\right)\right] (t>0,\ r\geq 0,\ z<0) \\ c(r,z,t) = c_0\ (z\to-\infty,\ \ t>0) \\ c(r,z,t) = c_0\ (z<0,\ \ t=0) \\ c(r,0,t) = 0\ \ (0\leq r\leq a(t),\ \ t>0) \\ \dfrac{\partial c}{\partial z}(r,0,t) = 0\ \ (r>a(t),\ \ t>0) \end{cases} \tag{8}$$

We consider the crack an ideal sink, with an atomic hydrogen concentration of 0. In general, it is known that this diffusion problem does not have solutions for a circular crack. However, it is possible to solve it first with a quasistationary approximation, where we assume the crack moves very slowly (long-time approximation); and second as a transient case, where we assume the crack moves very quickly (short-time approximation). We can then connect these two extreme cases through a Pade approximation.

3. Internal Crack Growth for Long Times

For the long-time approximation, we assume that the crack growth time t is much greater than the time to establish the stress equilibrium, or $a^2/D << t$, where a is the current crack radius and *D* is the gas Diffusion coefficient, and on each time step we can solve the stationary diffusion problem:

$$\begin{cases} \Delta c = 0 (t > 0,\ r \geq 0,\ z < 0) \\ c(r, z, t) = 0\ (z \to -\infty,\ \ t > 0) \\ c(r, 0, t) = -c_0\ \ (0 \leq r \leq a(t),\ \ t > 0) \\ \dfrac{\partial\, c}{\partial\, z}(r, 0, t) = 0\ \ \ (r > a(t),\ \ t > 0) \end{cases} \tag{9}$$

where we also subtracted the equilibrium gas distribution c_o. Solving this boundary-value problem for the derivative in the crack area, $r < a$, we can derive the gas flux inside the crack $q = -D\partial c/\partial z$ as follows (e.g., [32]):

$$q = \frac{2}{\pi} \cdot \frac{c_o D}{\sqrt{a(t)^2 - r^2}} \tag{10}$$

which can then be integrated over the area of the crack to find the total flux, *Q*:

$$Q = \int_0^{2\pi} \int_0^a q\, r dr d\theta = 4 c_o D a(t) \tag{11}$$

After substituting expression (10) into (7) the kinetic equation for the crack radius *a(t)* can be obtained in the form:

$$a^2 \gamma_c = \frac{3RTDc_o}{\pi} \int_0^t a(t)\, dt \tag{12}$$

The incubation time, t_i, which is the time it takes to reach the critical conditions at the crack contour, can be found from equation (12). The radius of the crack at that time is still a_0 and therefore does not depend on time and the integral can easily be taken, which yields the expression:

$$t_i = \frac{a_o \gamma_c \pi}{3RTDc_o} \tag{13}$$

After solving the integral equation, the expression for the crack radius a depending on time *t*, in the long-time approximation, can be obtained in closed form as follows:

$$a(t) = \frac{3RTDc_0}{2\gamma_c \pi} t + a_o \tag{14}$$

or in unidimensional form:

$$a'(t') = \frac{1}{2} t' + 1 \tag{15}$$

where the normalized crack radius, $a' = a/a_0$, and the normalized growth time, t/t_i (Figure 5). As equations (14) and (15) show, internal cracks propagate at a constant velocity. As gas diffuses into the crack, increasing the pressure, the crack also grows concurrently, increasing the volume. These two changes balance each other out, preventing the increasing gas pressure (from fluid diffusing into the crack) or the decreasing the gas pressure (from the increasing volume) from dominating. The result is smooth, constant-velocity crack growth. Slow crack growth, at constant speed, is typical for hydrogen embrittlement and confirmed by numerous experiments (e.g., [18, 33, 34]).

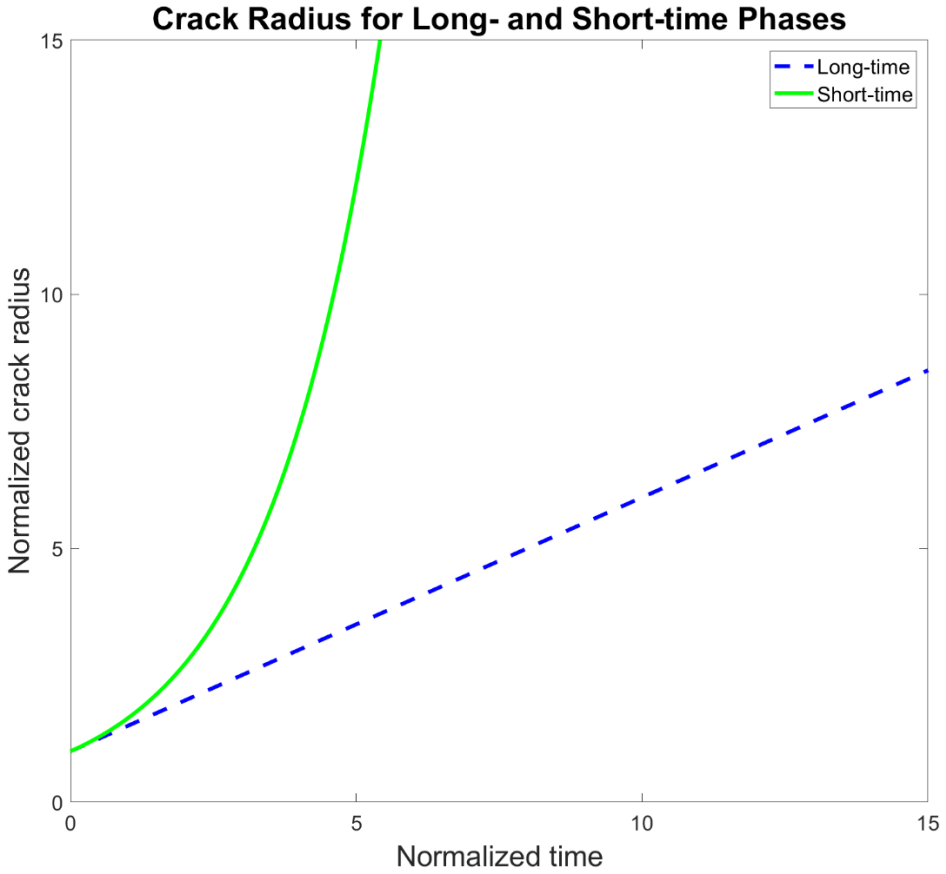

Figure 5 Normalized crack radius, $a' = a/a_0$, as a function of the normalized growth time, t/t_i, for short (solid line) and long (dotted line) times.

4. Internal Crack Growth for Short Times

The solution arrived at above is valid for a long-time approximation, where $t >> a^2/D$. It also provides an upper bound for growth time, $t(a)$. As mentioned earlier, the diffusion problem (8) in general cannot be solved in closed form but can only be solved numerically [35]. However, following Germanovich and Kill' [36], it is possible to obtain a closed form asymptotic solution for the transient diffusion into a growing fracture in the case of short times, $t << a^2/D$.

When the crack propagates quickly, the main contribution into the gas diffusion is provided by the flux in z-direction, whereas the flux in radial direction is less by one order of magnitude [37]. In this case, we can neglect the gas distribution in the radial direction and solve the boundary value problem (8) with the assumption that it does not depend on r [36], which makes it 1-dimensional approximation. The solution of the transient 1-dimensional diffusion problem is known (e.g., [38]):

$$c(z,t) = \begin{cases} -c_0 erf\,\frac{z}{2\sqrt{D\,t}} (r < a_0), \mathrm{erf}\,(x) = \frac{2}{\sqrt{\pi}} \int_0^x e^{-\eta^2} d\,\eta \\ 0 \quad (r > a_0) \end{cases} \tag{16}$$

Then the expression for the integral gas flux through the crack surfaces $q = -D\partial c/\partial z$ ($z = 0$, $0 \le r < a$) can be written:

$$q = \frac{c_o\sqrt{D}}{\sqrt{\pi t}} \tag{17}$$

and the total flux through the crack area is:

$$Q = \int_0^{2\pi} \int_0^{a(t)} q\, r dr d\theta = \frac{c_o a(t)^2 \sqrt{\pi D}}{\sqrt{t}} \tag{18}$$

Equation (7) is still true, although Q is now expressed by (18), and the kinetic equation of the growing crack with the radius $a(t)$ in short time approximation can be expressed as follows:

$$a^2\gamma_c = \frac{3c_o\sqrt{D}RT}{4\sqrt{\pi}} \int_0^t \frac{a(t)^2}{\sqrt{t}} dt \tag{19}$$

Taking into account that during the incubation time, t_i, the crack radius $a(t) = a_0$, we can easily integrate the right-hand side of the equation (19), which readily gives us the expression for the incubation time:

$$t_i = \frac{4{\gamma_c}^2\pi}{9{c_o}^2 D R^2 T^2} \tag{20}$$

After differentiating both sides of (19) and solving the differential equation, the closed form solution how the crack radius $a(t)$ changes with time t can be obtained in the form:

$$a(t) = a_o e^{\frac{3c_0 RT\sqrt{Dt}}{4\sqrt{\pi}\gamma_c}} \tag{21}$$

or in unidimensional form:

$$a'(t') = e^{\frac{1}{2}\sqrt{t'}} \tag{22}$$

The results show that in short-time approximation, $t << a^2/D$, the internal crack radius a grows exponentially with time. Note that since the accurate, higher-dimension solution was replaced with a 1-dimensional approximation (21) by neglecting higher-order terms, the gas influx into the crack, $Q(t)$, increases, which gives us a lower estimate for the crack growth time in the short-time approximation.

5. Analysis of Results and Pade Approximation

Closed-form solutions for the Hydrogen Induced internal crack incubation period, t_i, and growth time, t, have been obtained in the long, $a^2/D << t_i \le t$, and short, $t_i \le t << a^2/D$, time approximations

(Figure 5 and Figure 6). To choose which one of these asymptotics is applicable in each particular case, we should first compare the incubation periods (13) and (20) to the characteristic diffusion time scale, $t_0 = a_0^2/D$, where a_0 is the initial crack radius. If t_0 is smaller than t_i, an analytical formula (14) for the long-time approximation is applicable. Otherwise, expression (21) for short time should be used.

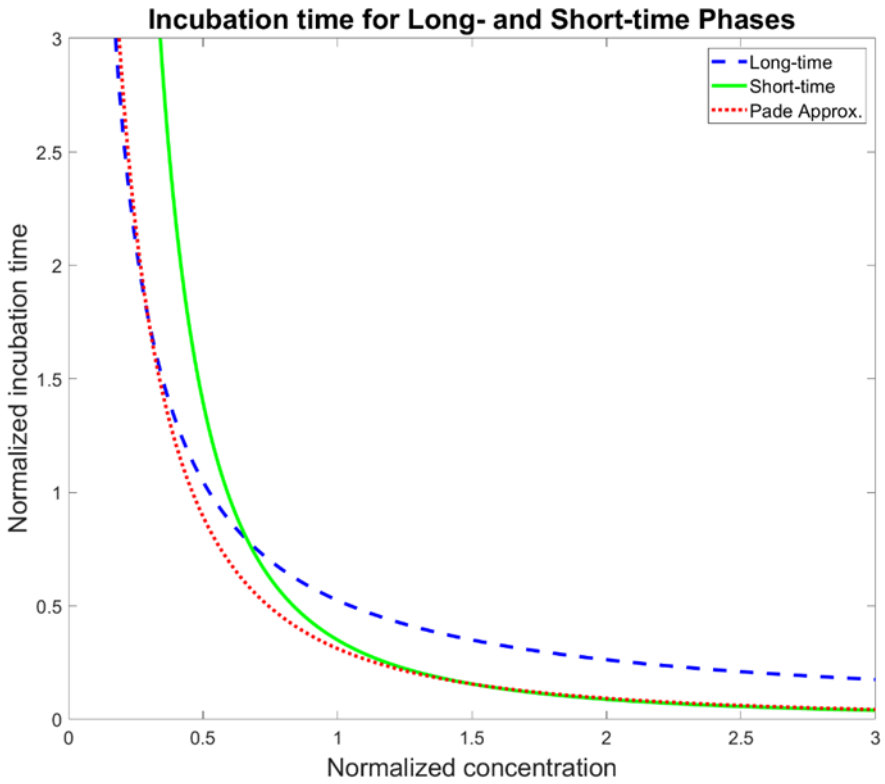

Figure 6 Normalized incubation time, $t' = t_i/t_0$, as a function of the normalized hydrogen concentration, $c' = c_0/c_*$, for short- and long-time approximations (solid and dotted curves correspondingly), and as a Padé approximation.

In Figure 5, the dependence of the normalized crack radius, $a' = a/a_0$, on the normalized growth time, t/t_i, is presented, for long (dotted line) and short (solid line) time approximations. Depending on the comparison of the growth time t with the characteristic diffusion time, $t_0 = a_0^2/D$, the long time or short time approximation should be chosen, and then either formula (14) or (21) should be used to estimate the longevity of the structure.

Figure 6 shows the dependence of the normalized incubation time, $t_i' = t_i/t_0$, on the dimensionless gas concentration in the material, $c_0' = c_0/c_*$, where $c_* = 2\gamma/(a_0 RT)$ and $t_0 = a_0^2/D$. Long-time (13) and short-time (20) approximations for the incubation times depending on hydrogen concentration can be rewritten correspondingly in the following unidimensional form

$$t_{il}' = \frac{\pi}{6c_o'} \tag{23}$$

for long times, and

$$t_{is}' = \frac{\pi}{9c_o'} \tag{24}$$

for short times. A dotted line and a solid line in Figure 6 correspond to the incubation times in the long- and short-time approximations, respectively. For these approximations to be applicable, t_i should not be too close to t_0. From a practical standpoint though, long- and short-time solutions are nearly equal near $t_i \approx t_0$ ($t_i' = 1$ in Figure 6) so that no interpolation is really needed between these approximations. However, if one wishes to have a single expression covering both cases, it can easily be done by using, for instance, a Padé asymptotic approximation (e.g., [39]). Then, the expression, which has the exact asymptotic properties for short and long times, can be written as

$$t_{ip}' = \frac{\pi}{6c_o' + 9{c_o}'^2 - A \cdot 3\sqrt{6}{c_o}'^{3/2}} \tag{25}$$

where A should be chosen on the intersection of both curves on the graph

$$t_{il}' = t_{is}' \tag{26}$$

which yields $A = \frac{2}{3}$, and thus, the final Padé approximation is:

$$t_{ip}' = \frac{\pi}{6c_o' + 9{c_o}'^2 - 2\sqrt{6}{c_o}'^{3/2}} \tag{27}$$

Similar considerations apply to the period of the crack growth. As (15) shows, in the long-time approximation, the crack grows with a constant velocity that does not depend on its radius, *a*, and thickness, *h*. The growth time, *t*, should now be compared to the characteristic relaxation time, $t_d = a^2/D$, which, contrary to t_0, is not a constant but, obviously, has a meaning of the diffusion time scale corresponding to the changing crack radius, a. For $t > t_d$, the hydrogen concentration, *c*, can be considered steady because the diffusion process has enough time to adjust the concentration for every crack growth increment. In contrast, for $t < t_d$, the diffusion process is essentially transient and cannot be considered stationary, which implies that the short time approximation should be used in this case.

From Figure 6 we can find the critical concentration that limits the use of the quasi-static solution, which is $c_0' \approx 0.75$, the point of the intersection of two curves, for long times and short times. For high hydrogen concentration, c_0', the incubation period becomes sufficiently short, so that the short-time approximation can be used (Figure 6). When the short-time approximation is valid for the incubation period, $t < t_i$, it will also be valid for further crack growth, $t > t_i$. In fact, it becomes more and more accurate because the crack grows faster than diffusion can relax the concentration gradient. The long-time solution is inapplicable in this case since $t < t_d$. For smaller initial concentration, c_0', longer time, t_i, is required for the crack to start growing because the same amount of gas hydrogen as before still needs to accumulate inside the initial crack.

6. Discussions

Expression (21) shows the radius of the hydrogen driven crack, *a(t)*, grows with time exponentially for short-time approximation, or for the last, fast, stage of the crack growth. In the long-time approximation, when the crack moves slowly, or at the initial stage, from our calculations the crack radius grows with time at a constant speed accordingly to the formula (14):

$$a(t) = \frac{1}{2\alpha} t \tag{28}$$

where

$$\alpha = \frac{\pi \gamma_c}{3RTc_0 D} \tag{29}$$

A very slow stable growth is typical for Hydrogen Induced Cracks (HIC), and it is confirmed by many experiments on hydrogen embrittlement (e.g., [40, 41]). In our model it corresponds to a long-time approximation, and formula (28) is of a primary interest in evaluating durability of the equipment operating in hydrogen environment.

The developed model will now be used for the analysis of kinetics of a penny-shaped crack growing in metal exploited in conditions of hydrogen embrittlement. The typical range of K_{Ic} for hydrogen charged steel is 1 to 70 MPa·m$^{1/2}$ (e.g., [42-44]). Using $2\gamma = \mathrm{K}_{\mathrm{Ic}}^2/(\mathrm{E}/(1-\mathrm{v}^2))$, we accept the somewhat intermediate, order-of-magnitude value of $\gamma_c \approx 5$ kJ/m^2.

Concentration of the atomic hydrogen c_0 in low alloy steel is observed to vary in the range of 10^{-9} to 10^{-5} mol/mm^3 according to (e.g., [45, 46]). Here, for model calculation, we assume c_0 be 10^{-8} mol/mm^3 (e.g., [47, 48]).

The coefficient of proton diffusion, D, for steel varies in the range of 10^{-10}-10^{-7} mm^2/sec according Beggs and Hahn [40] and Thomson [49], and in the range of 10^{-5} to 10^{-4} mm^2/sec according to Yokobori [50]. As described by Sunami et al. [45], Goldstein et al. [51] and [52], for low alloy steel, D, can be as high as 10^{-3} mm^2/sec. For this model we assume D = 10^{-6} mm^2/sec.

We will introduce just one example of calculations of the metal durability for typical properties of metals and hydrogen concentrations. From (28) the hydrogen crack is spreading at the speed:

$$v = \frac{1}{2\alpha} \tag{30}$$

and with chosen for the model calculations properties of the metal and T = 300 °K the hydrogen induced crack speed is v = 2.17 × 10^{-9} mm/sec, and the crack with the initial size of a = 1 mm reaches the radius of a = 10 mm during time t = 139 years. However, depending upon the parameters and properties of the metal and hydrogen concentration, the metal durability (life-to-failure) varies rather considerably, i.e., from hours to decades.

7. Conclusions

In this work, we obtained a closed-form solution for the diffusion-controlled axisymmetric *internal* fracture growth. In general, an analytical solution for a penny-shaped crack growth under gas diffusion does not exist. However, it is possible to solve it for two time scale approximations. First, the hydrogen induced crack grows at a slow pace, and the problem was solved in steady-state approximation. As time continues, hydrogen accumulates in the crack and increases the pressure to a point where the crack starts growing quickly and a long time approximation is no longer applicable. For very fast growth, a transient elastic-diffusion problem was solved in short approximation. In addition, a critical maximum gas concentration was found, when the long time approximation stops working, and a short-time approximation should be used. Even though we cannot solve the problem

for times between these extreme two-case scenarios, we can then combine these two asymptotic solutions through the Pade approximation, obtaining the complete curve showing incubation time for any time.

The obtained analytical solution gives a quick and robust estimate for the longevity of a pipeline. By evaluating the size of different defects by methods of nondestructive control and modeling them as circular defects with approximately the same area, we can evaluate how long it would take for the defect to reach a critical size, and make recommendations whether the piece of the pipeline needs to be replaced.

Closed form solutions for long and short times showed that the internal hydrogen induced crack grows differently at different time scales. For long time approximation, or for small hydrogen pressures inside the crack, it grows at a constant speed, which is confirmed by many experiments, and it could take tens or even hundreds of years for it to reach a critical size, depending on hydrogen concentration in metal and its properties. Then, with hydrogen accumulating and building up pressure, cracks accelerate and grow exponentially, which eventually would lead to the break of this piece of the pipeline. The estimate for the longevity of a pipeline based on the long-time approximation only always gives us the upper estimate, based on the *principal of maximum* for the steady-case diffusion problems compared to the transient ones (e.g., [53]).

In this paper, we do not take into account the influence of stresses on the gas flow. Even though it can be significant for high strength steels (e.g., [54]), most of the equipment operating under hydrogen embrittlement conditions are made of moderate strength steels, where this effect is negligible (e.g., [55]).

Acknowledgments

The research was done with partial support of RFBR grants No. 17-08-01579 and No. 17-08-01312 and of contract #AAAA-A17-117021310386-3.

Author Contributions

Alla Balueva: Methodology, Validation, Writing-Original draft preparation, Reviewing and Editing. **Ilia Dashevskiy:** Conceptualization, Methodology, Supervision. **Christian Sims:** Writing-Original draft preparation, Data curation, Recourses.

Competing Interests

The authors have declared that no competing interests exist.

References

1. Ayadi S, Charles Y, Gaspérini M, Lemaire IC, Botelho TD. Effect of loading mode on blistering in iron submitted to plastic prestrain before hydrogen cathodic charging. Int J Hydrogen Energy. 2017; 42: 10555-10567.
2. Djukic MB, Zeravcic VS, Bakic GM, Sedmak A, Rajicic B. Hydrogen damage of steels: A case study and hydrogen embrittlement model. Eng Fail Anal. 2015; 58: 485-498.

3. Chang Y, Lu W, Guénolé J, Stephenson LT, Szczpaniak A, Kontis P, et al. Ti and its alloys as examples of cryogenic focused ion beam milling of environmentally-sensitive materials. Nature Commun. 2019; 10: 942.
4. Quirós C, Mougenot J, Lombardi G, Redolfi M, Brinza O, Charles Y, et al. Blister formation and hydrogen retention in aluminium and beryllium: A modeling and experimental approach. Nucl Mater Energy. 2017; 12: 1178-1183.
5. Wang D, Lu X, Deng Y, Guo X, Barnoush A. Effect of hydrogen on nanomechanical properties in Fe-22Mn-0.6 C TWIP steel revealed by in-situ electrochemical nanoindentation. Acta Mater. 2019; 166: 618-629.
6. Dadfarnia M, Nagao A, Wang S, Martin ML, Somerday BP, Sofronis P. Recent advances on hydrogen embrittlement of structural materials. Int J Fract. 2015; 196: 223-243.
7. Gudla VC, Storm M, Palmer BC, Lewandowski JJ, Withers PJ, Holroyd NH, et al. Environmentally induced crack (EIC) initiation, propagation, and failure: A 3D in-situ time-lapse study of AA5083 H131. Corros Sci. 2020; 174: 108834.
8. Zamanzade M, Müller C, Velayarce JR, Motz C. Susceptibility of different crystal orientations and grain boundaries of polycrystalline Ni to hydrogen blister formation. Int J Hydrog Energy. 2019; 44: 7706-7714.
9. Chulkin SG, Zinovieva TV. Calculation of hydrogen influence on strength of marine pipeline. Mar Intellect Technol. 2019; 1: 31-35.
10. Huysmans S, De Bruycker E, Vanderlinden F. Complementary research related to SCC sensitivity of T24 boiler tubing. Part 2: Investigation of the hydrogen embrittlement susceptibility. ResearchGate. 2014. doi:10.13140/RG.2.2.16566.91200.
11. Zhang Y, Fan M, Xiao Z. Nonlinear elastic-plastic stress investigations on two interacting 3-D cracks in offshore pipelines subjected to different loadings. AIMS Mater Sci. 2016; 3: 1321-1339.
12. Benannoune S, Charles Y, Mougenot J, Gaspérini M, De Temmerman G. Numerical simulation by finite element modelling of diffusion and transient hydrogen trapping processes in plasma facing components. Nucl Mater Energy. 2019; 19: 42-46.
13. Benannoune S, Charles Y, Mougenot J, Gaspérini M, De Temmerman G. Multidimensional finite-element simulations of the diffusion and trapping of hydrogen in plasma-facing components including thermal expansion. Phys Scr. 2020; 2020: 014011.
14. Zhou H, Ye D, Chen J, Wang Q, Fan X. Discussion on the characterisation of hydrogen embrittlement based on eddy current signals. INSIGHT. 2020; 62: 11-14.
15. Gong P, Katzarov I, Nutter J, Paxton AT, Wynne B, Rainforth WM. Hydrogen suppression of dislocation cell formation in micro and nano indentation of pure iron single crystals. Scr Mater. 2021; 194: 113683.
16. Mai HL, Cui XY, Scheiber D, Romaner L, Ringer SP. An understanding of hydrogen embrittlement in nickel grain boundaries from first principles. Mater Des. 2021; 212: 110283.
17. Gibala R, Counts WA, Wolverton C. The hydrogen cold work peak in BCC iron: Revisited, with first principles calculations and implications for hydrogen embrittlement. Mater Res. 2018; 21. doi:10.1590/1980-5373-mr-2017-0868.
18. Ishikawa N, Ohmi T, Yokobori AT. Hydrogen diffusion analysis in the fatigue crack growth test under high pressure hydrogen. Proceedings of the ASME 2015 pressure vessels and piping conference; 2015 July 19-23; Boston, Mass, USA. New York: American Society of Mechanical Engineers.

19. Djukic MB, Bakic GM, Zeravcic VS, Rajicic B, Sedmak A, Mitrovic R, et al. Towards a unified and practical industrial model for prediction of hydrogen embrittlement and damage in steels. Procedia Struct Integr. 2016; 2: 604-611.
20. Müller C, Zamanzade M, Motz C. The impact of hydrogen on mechanical properties; a new in situ nanoindentation testing method. Micromachines. 2019; 10: 114.
21. Rajabipour A, Melchers RE. Application of Paris' law for estimation of hydrogen-assisted fatigue crack growth. Int J Fatigue. 2015; 80: 357-363.
22. Reinoso J, Paggi M, Rolfes R. A computational framework for the interplay between delamination and wrinkling in functionally graded thermal barrier coatings. Comput Mater Sci. 2016; 116: 82-95.
23. Sunnardianto GK, Bokas G, Hussein A, Walters C, Moultos OA, Dey P. Efficient hydrogen storage in defective graphene and its mechanical stability: A combined density functional theory and molecular dynamics simulation study. Int J Hydr Energy. 2021; 46: 5485-5494.
24. Vergani LM, Sciuccati A, Colombo C. A model to predict the hydrogen effect on crack growth rate in high-strength steels. Proceedings of the international hydrogen conference (IHC 2012): hydrogen-materials interactions; 2012 September 9-12; Moran, WY, USA. New York: ASME Press.
25. Martínez Pañeda E, Golahmar A, Niordson CF. A phase field formulation for hydrogen assisted cracking. Comput Methods Appl Mech Eng. 2018; 342: 742-761.
26. Huang S, Zhang Y, Yang C, Hu H. Fracture strain model for hydrogen embrittlement based on hydrogen enhanced localized plasticity mechanism. Int J Hydr Energy. 2020; 45: 25541-25554.
27. Toribio J, Kharin V. A generalised model of hydrogen diffusion in metals with multiple trap types. Philos Mag. 2015; 95: 3429-3451.
28. Wu W, Wang Y, Shen L, Gong J. Modeling of the slow crack growth caused by internal hydrogen in metals. Mater Sci. 2018; 54: 115-123.
29. Balueva AV, Dashevskiy IN. Growth of hydrogen delaminations in metals. Mech Solids. 1999; 34: 119-123.
30. Balueva AV. Asymptotic approach to the constant velocity of hydrogen delamination growth. Int J Mech Sci. 2008; 50: 22-29.
31. Balueva AV, Dashevskiy IN. Modeling of the gas-controlled crack growth: Non-ideal vs ideal sink. Proceedings of the ASME international mechanical engineering congress and exposition; 2016 November 11-17; Phoenix, AZ, USA. New York: American Society of Mechanical Engineers.
32. Sneddon IN. The use of integral transforms. New York: McGraw Hill; 1972.
33. Moody NR, Robinson SL, Perra MW. Internal hydrogen effects on thresholds for crack growth in the iron-based superalloy IN903. Eng Fract Mech. 1991; 39: 941-954.
34. Singh S, Altstetter C. Effects of hydrogen concentration on slow crack growth in stainless steels. Metall Trans A. 1982; 13: 1799-1808.
35. Balueva AV. 3D problems of cracks kinetics due to gas diffusion. Mech Solids. 1993; 6: 123-131.
36. Germanovich LN, Kill ID. Convective heating of a half-space (nonsymmetric case). J Eng Phys. 1985; 48: 113-114.
37. Germanovich LN. Temperature stresses in an elastic half space with heat sources. Mech Solids. 1986; 21: 77-88.
38. Carslaw HS, Jaeger JC. Conduction of heat in solids. 2nd ed. Oxford: Clarendon Press; 1992.

39. Baker GA Jr, Graves Morris PR. Pade approximants. 2nd ed. Cambridge: Cambridge University Press; 1996.
40. Beggs DV, Hahn MT. Recent observation on the propagation of stress corrosion cracks and their relevance to proposed mechanisms of stress corrosion cracking. In: Hydrogen embrittlement and stress corrosion cracking. Metal Park: ASM; 1984. pp.181-205.
41. Shiraiwa T, Kawate M, Briffod F, Kasuya T, Enoki M. Evaluation of hydrogen-induced cracking in high-strength steel welded joints by acoustic emission technique. Mater Design. 2020; 190: 108573.
42. Strnadel B. Failure of steels caused by hydrogen induced microcracking. Eng Fract Mech. 1998; 61: 299-310.
43. Brown BF. Stress corrosion cracking in high strength steels and titanium and aluminum alloys. Washington: Naval Research Laboratory; 1972.
44. Agarwala VS. Modification of crack-tip chemistry to inhibit corrosion and stress corrosion cracking in high strength alloys. J Metals. 1983; 35: A61.
45. Sunami E, Tanimura M, Tenmyo G. Behavior and thermodynamical properties of tantalim-carbide and -nitride in steels. Boshoku Gijutsu. 1974; 23: 281-287.
46. Yen SK, Tsai YC. Critical hydrogen concentration for the brittle fracture of AISI 430 stainless steel. J Electrochem Soc. 1996; 143: 2736-2741.
47. Zakroczymski T, Glowacka A, Swiatnicki W. Effect of hydrogen concentration on the embrittlement of a duplex stainless steel. Corros Sci. 2005; 47: 1403-1414.
48. Addach H, Bercot P, Rezrazi M, Wery M. Hydrogen permeation in iron at different temperatures. Mater Lett. 2005; 59: 1347-1351.
49. Thompson AW. Current status of the role of hydrogen in stress corrosion cracking. Mater Sci Eng. 1980; 43: 41-46.
50. Yokobori AT. The mechanism of hydrogen embrittlement: The stress interaction between a crack, a hydrogen cluster, and moving dislocations. Int J Fract. 2004; 128: 121-131.
51. Goldstein RV, Entov VM, Pavlovsky BR. Model of development of hydrogen cracks in metal. Dokl Akad Nauk SSSR. 1977; 237: 828-831.
52. Goldstein RV, Zazovskii AF, Pavlovsky BR. Development of penny-shaped layering in a metal sheet. Fis Khim Mekh Mater. 1985; 21: 621-656.
53. Garabedian PR. Partial differential equations. Rhode Island: AMS Chelsea Publishing; 1986.
54. Yokobori Jr AT, Nemoto T, Satoh K, Yamada T. Numerical analysis on hydrogen diffusion and concentration in solid with emission around the crack tip. Eng Fract Mech. 1996; 55: 47-60.
55. Gerberich WW, Chen YT, John C. A short-time diffusion correlation for hydrogen-induced crack growth kinetics. Metall Trans A. 1975; 6: 1485-1498.

Enjoy *JEPT* by:

1. Submitting a manuscript
2. Joining in volunteer reviewer bank
3. Joining Editorial Board
4. Guest editing a special issue

For more details, please visit:
http://www.lidsen.com/journal/jept